Proceedings of the ASME 2007 International Design Engineering Technical Conferences & Computers and Information in Engineering Conference
IDETC/CIE 2007
September 4-7, 2007 Las Vegas, Nevada, USA

DETC2007-34433

REVERSE KINEMATIC ANALYSIS OF THE SPATIAL SIX AXIS ROBOTIC MANIPULATOR WITH CONSECUTIVE JOINT AXES PARALLEL

Javier Roldán Mckinley
Center for Intelligent Machines and Robotics
University of Florida,
Gainesville, Florida, USA
mckinrold@yahoo.com

Carl Crane III*
Center for Intelligent Machines and Robotics
University of Florida
Gainesville, Florida, USA
ccrane@ufl.edu

David B. Dooner
University of Puerto Rico at Mayagüez
Mayagüez, Puerto Rico
d_dooner@me.uprm.edu

ABSTRACT

This paper introduces a reconfigurable one degree-of-freedom spatial mechanism that can be applied to repetitive motion tasks. The concept is to incorporate five pairs of non-circular gears into a six degree-of–freedom closed-loop spatial chain. The gear pairs are designed based on the given mechanism parameters and the user defined motion specification of a coupler link of the mechanism. It is shown in the paper that planar gear pairs can be used if the spatial closed-loop chain is comprised of six pairs of parallel joint axes, i.e. the first joint axis is parallel to the second, the third is parallel to the fourth, …, and the eleventh is parallel to the twelfth. This paper presents the detailed reverse kinematic analysis of this specific geometry. A numerical example is presented.

Keywords: Robotic manipulators; spatial kinematics; spherical mechanism; reverse kinematic analysis; non-circular gears.

1. INTRODUCTION

The reverse kinematic analysis of spatial mechanisms has been widely studied for practically any combination of revolute, cylindrical, and prismatic joints, see [1]-[16]. Many solution techniques were investigated to obtain the reverse kinematic analysis. Duffy and Rooney [15] introduced a unified theory for the analysis of spatial mechanisms which was utilized on many cases (Crane and Duffy [16]). Other solution techniques include numerical iteration and continuation methods [17]-[21]. The approach used in this paper, based on the unified theory, has the advantage in that solutions are obtained without the requirement for any iterations or initial guess values.

The 7R mechanism is the most complicated kinematic analysis of a one degree of freedom spatial loop and this was referred to as the "Mount Everest of kinematic problems" by Professor Ferdinand Freudenstein. Duffy and Crane [22] obtained a 32^{nd} degree input-output equation in the tan-half-angle of the output angular displacement for this mechanism. Lee and Liang [23] later obtained a 16^{th} degree polynomial input-output equation in the tan-half-angle of the output angular displacement. More recently, Husty, Pfurner and Schröcker [24] used multidimensional geometry and Segre manifolds' theory to interpret the nature of the general 6R-chains reverse kinematic problem.

This paper presents the solution of a spatial 7R closed-loop mechanism with consecutive pairs of joint axes parallel. The motivation of this work is related to future applications of spatial motion generation incorporating non-circular gears. Fig. 1(a) shows a planar motion generator where two pairs of non-circular gears have been designed in order to attain a desired motion of the coupler link of a six link mechanism. Fig. 1(b) shows an extension of this concept to the spatial case. Five pairs of non-circular gears have been designed and incorporated in a twelve link closed-loop chain to obtain a one degree-of-freedom mechanism where the coupler link (containing point P) follows a desired motion profile. Planar non-circular gears can be utilized if adjacent joint axes are parallel as shown in Fig. 1(b). The closed-loop mechanism can be separated into two six-axis open-loop mechanisms. A reverse kinematic analysis of this device is required in order to design the non-circular gears that will position the distal link as desired for the specified

* Professor and author of correspondence, Phone: (352) 392-9461, Fax: (352) 392-1071, Email: ccrane@ufl.edu.

motion profile. This paper details the reverse kinematic analysis of this particular six axis open-loop chain. The special geometry is that the 1st and 2nd axes are parallel, the 3rd and 4th axes are parallel, and the 5th and 6th joint axes are parallel.

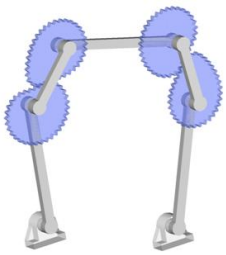

(a) planar case

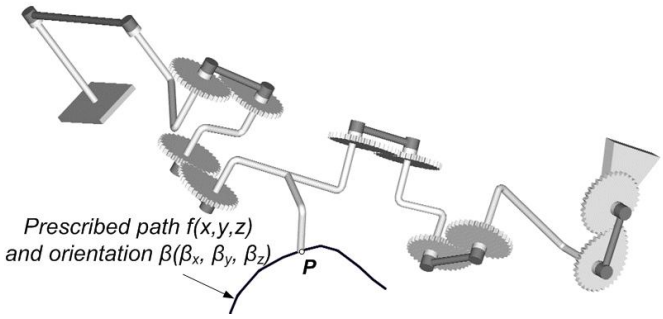

(b) spatial case

Figure 1: Incorporation of planar non-circular gears into (a) planar mechanism and (b) spatial mechanism to obtain one degree of freedom motion generation.

2. NOMENCLATURE

a_{ij}	=	Link distance of the i link
S_i	=	Offset distance of the i link
θ_i	=	Joint angle of the i link
α_{ij}	=	Twist angles of the i link
φ_1	=	Angle between the x axes of the fixed and 1st coordinate systems
γ_1	=	Angle between the x axes of the hypothetical link coordinate system and the fixed coordinate system
$\mathbf{a}_{ij}$	=	Link unit vector of the i link
$\mathbf{S}_i$	=	Joint unit vector of the i link
$\mathbf{P}$	=	Position vector
$\mathbf{R}$	=	Rotation matrix
$\mathbf{i}, \mathbf{j}, \mathbf{k}$	=	Unit vectors along the x y z axes
s_i, c_i	=	Sine and cosine of the joint angle θ_i
s_{ij}, c_{ij}	=	Sine and cosine of the twist angle α_{ij}
s_{i+j}, c_{i+j}	=	Sine and cosine of the sum of angles $\theta_i + \theta_j$

3. REVERSE KINEMATIC ANALYSIS

3.1 Problem Statement

Figure 2 presents the joint vectors, link vectors and joint angles labeling corresponding to an open-loop six axis chain with consecutive joint axes parallel: $\mathbf{S}_1 \| \mathbf{S}_2$, $\mathbf{S}_3 \| \mathbf{S}_4$ and $\mathbf{S}_5 \| \mathbf{S}_6$. The problem statement for the mechanism is summarized as

Given

1). The constant mechanism parameters:
link distances a_{12}, a_{23}, a_{34}, a_{45}, a_{56}
twist angles $\alpha_{12}=0$, α_{23}, $\alpha_{34}=0$, α_{45}, $\alpha_{56}=0$
offset distances S_2, $S_3=0$, S_4, $S_5=0$.

2) User defined parameters to establish the 6th coordinate system, i.e. the coordinate system attached to the last link:
distance S_6 and direction of vector $\mathbf{a}_{67}$ relative to link offset S_6

3). Tool point measured in the 6th coordinate system: ${}^6\mathbf{P}_{tool}$

4). Desired location of tool point as measured in the fixed coordinate system: ${}^F\mathbf{P}_{tool}$

5). Desired orientation of the end effector link as measured in the fixed coordinate system: ${}^F\mathbf{S}_6$ and ${}^F\mathbf{a}_{67}$

Find

The joint angle parameters φ_1, θ_2, θ_3, θ_4, θ_5, and θ_6 that will position and orient the last link as specified.

3.2 Determination of Equivalent Closed-Loop Spatial Mechanism

The solution method for this problem follows the approach defined in Crane and Duffy [16]. First the coordinates of the origin point of the 6th coordinate system are calculated as

$$ {}^F\mathbf{P}_{6orig} = {}^F\mathbf{P}_{tool} - ({}^6\mathbf{P}_{tool} \cdot \mathbf{i}){}^F\mathbf{a}_{67} - ({}^6\mathbf{P}_{tool} \cdot \mathbf{j}){}^F\mathbf{S}_6 \times {}^F\mathbf{a}_{67} - ({}^6\mathbf{P}_{tool} \cdot \mathbf{k}){}^F\mathbf{S}_F. \quad (1) $$

At this point the 4x4 transformation matrix that describes the position and orientation of the 6th coordinate system with respect to ground, ${}^F_6\mathbf{T}$, is known since the fourth column of the matrix is defined by ${}^F\mathbf{P}_{6orig}$ and the columns of the upper 3×3 sub-matrix are defined by ${}^F\mathbf{a}_{67}$, ${}^F\mathbf{S}_6 \times {}^F\mathbf{a}_{67}$ and ${}^F\mathbf{S}_6$. Thus

$$ {}^F_6\mathbf{T} = \left[\begin{array}{ccc|c} & {}^F_6\mathbf{R} & & {}^F\mathbf{P}_{6orig} \\ \hline 0 & 0 & 0 & 1 \end{array}\right] \quad (2) $$

where:

$$ {}^F_6\mathbf{R} = [{}^F\mathbf{a}_{67} \;\; {}^F\mathbf{S}_6 \times {}^F\mathbf{a}_{67} \;\; {}^F\mathbf{S}_6]. \quad (3) $$

Next, a hypothetical seventh joint axis is defined by arbitrarily selecting values for the parameters a_{67} and α_{67}. The selected values for these parameters are

$$ a_{67}=0 \quad (4) $$

$$ \alpha_{67}=90°. \quad (5) $$

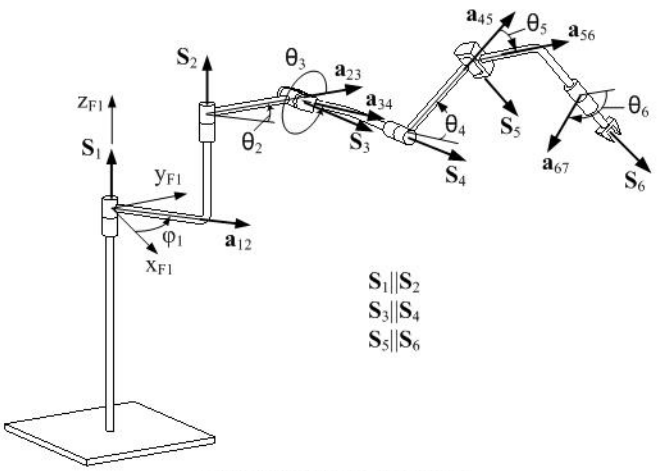

(a) Joint angles labeling

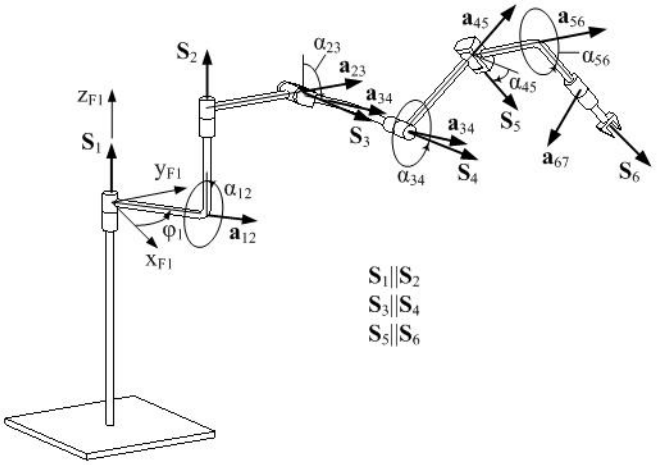

(b) Link angles labeling

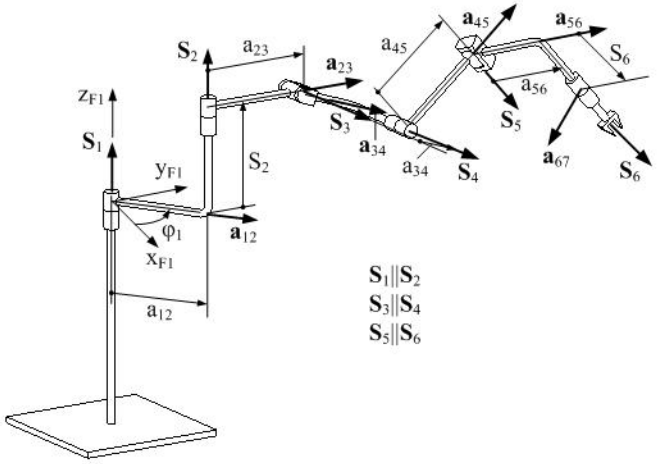

(c) Link and offset distances labeling

Figure 2: Joint vectors, link vectors and joint angles of the open-loop spatial mechanism.

A hypothetical link (see Figure 3) is then inserted between the new seventh joint axis and the first joint axis. Three distances, S_7, a_{71}, and S_1 and three angles, α_{71}, θ_7, and γ_1 are then readily determined as described in [16]. The angle γ_1 is shown in Figure 3 and its relation to θ_1 can be written as

$$\theta_1 = \varphi_1 + \gamma_1. \quad (6)$$

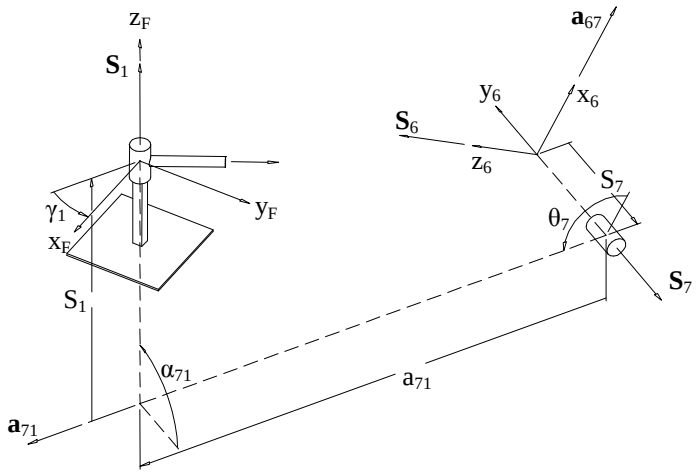

Figure 3: Hypothetical closure link

At this point an equivalent closed-loop spatial mechanism, formed by seven links and seven revolute joints, has been defined where all the link lengths, a_{12} through a_{71}, all the twist angles, α_{12} through α_{71}, and all the joint offsets, S_1 through S_7, are known. Further the resulting closed-loop mechanism is a one degree-of-freedom device where the angle θ_7 is known.

3.3 Equivalent Spherical Mechanism

Crane and Duffy [16] solve closed-loop spatial mechanisms by introducing sine, sine-cosine, and cosine laws for an equivalent spherical mechanism that is associated with the closed-loop mechanism. These laws provide expressions that contain only the joint angles and twist angles of the spatial mechanism. An equivalent closed-loop spherical mechanism can be formed from the closed-loop spatial mechanism by translating the directions of the joint axis vectors and the link vectors so that they all intersect at a point. Spherical links may be inserted on a unit sphere to maintain the angular relationships between the joint axis vectors. The equivalent spherical mechanism for the case under consideration is shown in Figure 4. The equivalent spherical mechanism has reduced to a quadrilateral since the spatial mechanism has adjacent axes parallel.

A spherical quadrilateral is a one degree-of-freedom mechanism (further information about mobility see Real *et al* [26]). In this case θ_7 is known and it is thus possible to obtain solutions for the remaining angles of the spherical quadrilateral which in this case are the three sums $\theta_1+\theta_2$, $\theta_3+\theta_4$, and $\theta_5+\theta_6$.

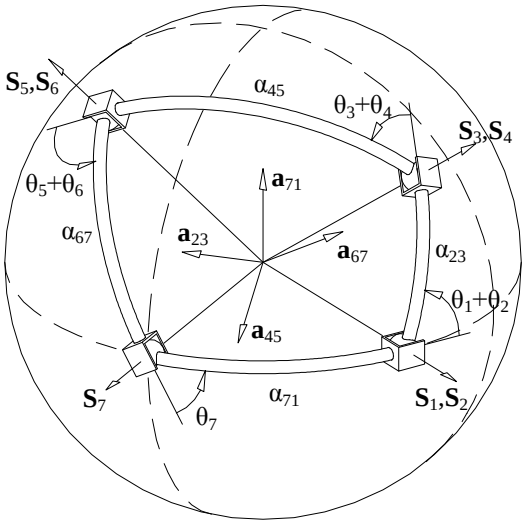

Figure 4: Equivalent spherical quadrilateral.

3.4 Solution of Spherical Quadrilateral

The solution starts with solving the spherical quadrilateral depicted in Figure 4 to find the sums of the angles $\theta_1+\theta_2$, $\theta_3+\theta_4$, and $\theta_5+\theta_6$. A detailed solution is presented in [16] which also presents a derivation of the sine, sine-cosine, and cosine laws for a spherical quadrilateral that will be used here.

3.4.1 Solving for $\theta_1+\theta_2$

A spherical cosine law may be written that will relate the angle θ_7 and the joint angle sum $\theta_1+\theta_2$. This cosine law is written here as

$$A\,C_{1+2} + B\,S_{1+2} + D = 0 \qquad (7)$$

where s_{i+j} and c_{i+j} represent the sine and cosine of the sum $\theta_i+\theta_j$ and where

$$A = -s_{23}\,(s_{71}\,c_{67} + c_{71}\,s_{67}\,c_7)$$

$$B = s_{23}\,s_{67}\,s_7$$

$$D = c_{23}\,(c_{71}\,c_{67} - s_{71}\,s_{67}\,c_7).$$

The terms s_{ij} and c_{ij} represent the sine and cosine of the twist angle α_{ij} and the terms s_i and c_i represent the sine and cosine of the joint angle θ_i. Equation (7) can be solved for two solutions for θ_{1+2} which will be referred to as $\theta_{(1+2)A}$ and $\theta_{(1+2)B}$, where $\theta_{(i+j)}= \theta_i+\theta_j$.

3.4.2 Solving for $\theta_3+\theta_4$

Corresponding values for the sum $\theta_3+\theta_4$ can be determined from a sine and sine-cosine law for the equivalent spherical quadrilateral. These equations are written as

$$s_{3+4} = \frac{1}{s_{45}}\left[(s_{67}s_7)c_{1+2} + (s_{71}c_{67} + c_{71}s_{67}c_7)s_{1+2}\right] \qquad (8)$$

$$c_{3+4} = \frac{1}{s_{45}}\left[c_{23}\,A_{34} - s_{23}(c_{71}c_{67} - s_{71}s_{67}c_7)\right] \qquad (9)$$

where:

$$A_{34} = (s_{67}s_7)s_{1+2} - (s_{71}c_{67} + c_{71}s_{67}c_7)c_{1+2}.$$

The corresponding values for $\theta_{(3+4)A}$ and $\theta_{(3+4)B}$ for each value of θ_{1+2} are obtained from (8) and (9).

3.4.3 Solving for $\theta_5+\theta_6$

Corresponding values for the sum $\theta_5+\theta_6$ can be determined from the following sine and sine-cosine laws:

$$s_{5+6} = \frac{1}{s_{45}}\left[(s_{23}s_{1+2})c_7 + (s_{71}c_{23} + c_{71}s_{23}c_{1+2})s_7\right] \qquad (10)$$

$$c_{5+6} = \frac{1}{s_{45}}\left[c_{67}A_{56} - s_{67}(c_{71}c_{67} - s_{71}s_{67}c_7)\right] \qquad (11)$$

where:

$$A_{56} = (s_{23}s_{1+2})s_7 - (s_{71}c_{23} + c_{71}s_{23}c_{1+2})c_7.$$

The corresponding values for θ_{5+6} are obtained from (10) and (11) for each value of θ_{1+2}.

At this point of the analysis, two values for θ_{1+2} and unique corresponding values for the sums θ_{3+4} and θ_{5+6} have been determined. A solution tree of the sum of angles solution is presented in Fig 5.

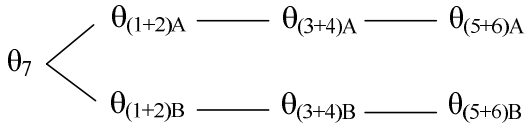

Figure 5: Solution tree of the spherical quadrilateral to find the sums of consecutive angle joints

3.5 Spatial Mechanism Joint Angles

In this section, the individual joint angles θ_1 through θ_6 are obtained from projections of the vector loop equation of the spatial mechanism and from knowledge of the sums of angles that have been previously determined.

3.5.1 Vector Loop Equation

The vector loop equation for the equivalent closed-loop mechanism is written as

$$S_1\mathbf{S}_1 + a_{12}\mathbf{a}_{12} + S_2\mathbf{S}_2 + a_{23}\mathbf{a}_{23} + a_{34}\mathbf{a}_{34} + S_4\mathbf{S}_4 + a_{45}\mathbf{a}_{45} + a_{56}\mathbf{a}_{56} + S_6\mathbf{S}_6 + S_7\mathbf{S}_7 + a_{71}\mathbf{a}_{71} = \mathbf{0}. \qquad (12)$$

The vector terms will all be evaluated in terms of a right-handed coordinate system whose Z axis is along $\mathbf{S}_3$ and whose X axis is along $\mathbf{a}_{23}$. This yields the following three equations:

$$A_1c_2+A_2c_3+A_3c_5+A_4s_5+A_5 = 0, \qquad (13)$$

$$B_1s_2+B_2s_3+B_3c_5+B_4s_5+B_5 = 0, \qquad (14)$$

$$D_1s_2+D_2s_5+D_3 = 0 \qquad (15)$$

where the coefficients A_1 through D_3 can be expressed in terms of known quantities as

$$A_1 = a_{12},\ A_2 = a_{34},\ A_3 = a_{56}c_{3+4},\ A_4 = -a_{56}c_{45}s_{3+4},$$

$$A_5 = S_7s_{71}s_{1+2} + S_6(c_{71}c_7s_{1+2}+s_7c_{1+2}) + a_{23} + a_{71}c_{1+2} + a_{45}c_{3+4},$$

$B_1 = -a_{12}c_{23}$, $B_2 = a_{34}$, $B_3 = a_{56}s_{3+4}$, $B_4 = a_{56}c_{45}c_{3+4}$,

$B_5 = S_2s_{23} + S_1s_{23} + S_7(s_{23}c_{71}+c_{23}s_{71}c_{1+2}) +$

$S_6[c_{23}(-s_7s_{1+2}+c_{71}c_7c_{1+2}) - s_{23}s_{71}c_7] - a_{71}c_{23}s_{1+2} + a_{45}s_{3+4}$,

$D_1 = a_{12}s_{23}$, $D_2 = a_{56}s_{45}$,

$D_3 = S_2c_{23} + S_1c_{23} + S_7(c_{23}c_{71}-s_{23}s_{71}c_{1+2}) +$

$S_6[s_{23}(s_7s_{1+2}-c_{71}c_7c_{1+2}) - c_{23}s_{71}c_7] + a_{71}s_{23}s_{1+2} + S_4.$ (16)

The known sums of angles θ_{1+2}, θ_{3+4}, and θ_{5+6} have been introduced in the terms c_{i+j} and s_{i+j} in the coefficients A_1 through D_3. In the next sections, equations (13) through (15) are solved for the three joint angles θ_2, θ_3 and θ_5.

3.5.2 Solution for θ_5 and θ_6

In this section equations (13), (14), and (15) are manipulated in order to obtain one equation in terms of the unknown sine and cosine of θ_5. Equation (13) can be solved for c_3 and (14) for s_3 to yield

$$c_3 = \frac{-A_1c_2 - A_3c_5 - A_4s_5 - A_5}{A_2} \quad (17)$$

$$s_3 = \frac{-B_1s_2 - B_3c_5 - B_4s_5 - B_5}{B_2}. \quad (18)$$

Squaring (17) and (18) and adding the two yields the following equation in terms of the two unknowns θ_2 and θ_5

$$\frac{(A_1c_2 + A_3c_5 + A_4s_5 + A_5)^2}{A_2^2} + \frac{(B_1s_2 + B_3c_5 + B_4s_5 + B_5)^2}{B_2^2} - 1 = 0. \quad (19)$$

Multiplying Eq. (19) by $(A_2B_2)^2$ and expanding gives

$$E_1c_2^2+E_2c_2+E_3s_2^2+E_4s_2+E_5 = 0 \quad (20)$$

where

$E_1 = A_1^2B_2^2$

$E_2 = E_{2A}c_5+E_{2B}s_5+E_{2c}$, $E_3 = A_2^2B_1^2$

$E_4 = E_{4A}c_5+E_{4B}s_5+E_{4C}$

$E_5 = E_{5A}c_5^2+E_{5B}s_5^2+E_{5C}s_5c_5+E_{5D}c_5+E_{5E}s_5+E_{5F}$, (21)

and where

$E_{2A} = 2A_1B_2^2A_3$, $E_{2B} = 2A_1B_2^2A_4$, $E_{2C} = 2A_1B_2^2A_5$,

$E_{4A} = 2B_1A_2^2B_3$, $E_{4B} = 2B_1A_2^2B_4$, $E_{4C} = 2B_1A_2^2B_5$,

$E_{5A} = A_2^2B_3^2+B_2^2A_3^2$, $E_{5B} = A_4^2B_2^2+B_4^2A_2^2$,

$E_{5C} = 2(A_3A_4B_2^2 + B_3B_4A_2^2)$,

$E_{5D} = 2(A_3A_5B_2^2 + B_3B_5A_2^2)$, $E_{5E} = 2(A_4A_5B_2^2 + B_4B_5A_2^2)$,

$E_{5F} = B_2^2(A_5^2-A_2^2) + A_2^2B_5^2$. (22)

Solving Eq. (15) for s_2 gives

$$s_2 = \frac{-D_2s_5 - D_3}{D_1}. \quad (23)$$

Squaring Eq. (23), substituting $s_2^2=1-c_2^2$ and solving for c_2^2 gives

$$c_2^2 = 1-\left(\frac{-D_2s_5 - D_3}{D_1}\right)^2. \quad (24)$$

Substituting (23) and (24) into (20) and regrouping gives

$$E_1\left[1-\left(\frac{-D_2s_5 - D_3}{D_1}\right)^2\right] + E_3\left(\frac{-D_2s_5 - D_3}{D_1}\right)^2 + E_4\left(\frac{-D_2s_5 - D_3}{D_1}\right) + E_5 = -E_2c_2. \quad (25)$$

Squaring (25) and substituting (24) for c_2^2 yields an equation in the sine and cosine of θ_5 which is written as

$F_1 s_5^4 + F_2 s_5^3 + F_3 s_5^3c_5 + F_4 s_5^2c_5^2 + F_5 s_5c_5^2 + F_6 c_5^2 +$
$F_7 s_5^2c_5 + F_8s_5c_5 + F_9 c_5 + F_{10} s_5^2 + F_{11} s_5 + F_{12} = 0$ (26)

where

$F_1 = D_2^2(D_1^2E_{4B}^2+D_1^2E_{2B}^2-2D_2E_3D_1E_{4B}+D_2^2E_3^2+$
$2D_2E_1D_1E_{4B}+D_2^2E1^2-2D_2^2E_1E_3)$

$F_2 = 2D_2(2D_2^2D_3E_1^2-4D_2^2D_3E_3E_1+2D_2^2D_3E_3^2-D_2^2E_3D_1E_{4C}+$
$D_2^2E_1D_1E_{4C}+D_2D_1^2E_{2B}E_{2C}-3D_2E_3D_1E_{4B}D_3+$
$D_2D_1^2E_{4B}E_{4C}+3D_2E_1D_1E_{4B}D_3+D_1^2E_{2B}^2D_3+D_1^2E_{4B}^2D_3$

$F_3 = 2D_2^2D_1(-D_2E_{4A}E_3+D_2E_{4A}E_1+D_1E_{2A}E_{2B}+D_1E_{4B}E_{4A})$

$F_4 = D_1^2D_2^2\ (E_{4A}^2+E_{2A}^2)$

$F_5 = 2D_1^2D_2D_3(E_{4A}^2+E_{2A}^2)$

$F_6 = D_1^2(D_1^2E_{2A}^2+E_{4A}^2D_3^2+E_{2A}^2D_3^2)$

$F_7 = 2D_1D_2(D_1D_2E_{2A}E_{2C}+D_1D_2E_{4A}E_{4C}-3D_2E_3E_{4A}D_3+$
$3D_2E_1E_{4A}D_3+2D_1E_{2A}E_{2B}D_3+2D_1E_{4A}E_{4B}D_3)$,

$F_8 = 2D_1(-E_{2A}E_{2B}D^3-D_1^2E_{4A}D_2E_5-D_1^2D_2E_{4A}E_1+$
$D_1E_{2A}E_{2B}D_3^2+D_1E_{4A}D_3^2E_{4B}+2D_1E_{2A}E_{2C}D_2D_3+$
$2D_1E_{4A}D_2E_{4C}D_3+3E_1D_2D_3^2E_{4A}-3E_3D_2D_3^2E_{4A})$

$F_9 = 2D_1(-E_{2A}E_{2C}D_1^3-D_1^2E_1E_{4A}D_3-D_1^2E_{4A}D_3E_5+$
$D_1E_{4A}D_3^2E_{4C}+D_1E_{2A}E_{2C}D_3^2+E_1D_3^3E_{4A}-E_3D_3^3E_{4A})$

$F_{10} = D_2^2[(6E_3^2+6E_1^2-12E_1E_3)D_3^2+(6E_1D_1E_{4C}-$
$6E_3D_1E_{4C})D_3-2E_1E_5D_1^2+D_1^2E_{2C}^2+ D_1^2E_{4C}^2-2E_1^2D_1^2 +$
$2E_1D_1^2E_3 + 2E_3E_5D_1^2]$
$+D_2[(6E_1D_1E_{4B}-6E_3D_1E_{4B})D_3^2+$
$(4D_1^2E_{2B}E_{2C}+4D_1^2E_{4B}E_{4C})D_3-2D_1^3E_{4B}E_5-$
$2E_1D_1^3E_{4B}]+(D_1^2E_{4B}^2+D_1^2E_{2B}^2)D_3^2 - D_1^4E_{2B}^2$

$F_{11} = D_2[(4E_1^2+4E_3^2-8E_1E_3)D_3^3+(6E_1D_1E_{4C}-6E_3D_1E_{4C})D_3^2$
$+(4E_1D_1^2E_3-4E_1E_5D_1^2+2D_1^2E_{4C}^2+2D_1^2E_{2C}^2-$
$4E_1^2D_1^2+4E_3E_5D_1^2)D_3-2E_1D_1^3E_{4C}-2D_1^3E_{4C}E_5]+$
$(2E_1D_1E_{4B}-2E_3D_1E_{4B})D_3^3+$
$2D_1^2E_{2B}E_C+2D_1^2E_{4B}E_{4C})D_3^2-$
$(2D_1^3E_{4B}E_5+2E_1D_1^3E_{4B})D_3 - 2D_1^4E_{2B}E_{2C}$

$F_{12} = D_3^4(E_1^2+E_3^2-2E_1E_3)+D_3^3(2E_1D_1E_{4C}-2E_3D_1E_{4C})+$
$D_3^2(D_1^2E_{2C}^2+D_1^2E_{4C}^2-2E_1E_5D_1^2-$
$2E_1^2D_1^2+2E_1D_1^2E_3+2E_3E_5D_1^2)-$
$D_3(2E_1D_1^3E_{4C}+2D_1^3E_{4C}E_5)+E_5^2D_1^4+2E_1D_1^4E_5+ E_1^2D_1^4$
$- D_1^4E_{2C}^2$. (27)

The tan-half angle of θ_5 is now introduced as

$$x_5 = \tan\left(\frac{\theta_5}{2}\right), \tag{28}$$

and the sine and cosine of θ_5 may be written in terms of x_5 via the trig identities

$$s_5 = \frac{2x_5}{1+x_5^2} \tag{29}$$

$$c_5 = \frac{1-x_5^2}{1+x_5^2}. \tag{30}$$

Substituting (29) and (30) into (26), dividing throughout by $(1+x_5^2)^4$, and regrouping yields

$$C_8x_5^8 + C_7x_5^7 + C_6x_5^6 + C_5x_5^5 + C_4x_5^4 + C_3x_5^3 + C_2x_5^2 + C_1x_5 + C_0 = 0 \tag{31}$$

where

$C_8 = F_{12} + F_6 - F_9$
$C_7 = 2\,(F_5 - F_8 + F_{11})$
$C_6 = 2\,(2F_4 - 2F_7 - F_9 + 2F_{10} + 2F_{12})$
$C_5 = 2\,(4F_2 - 4\,F_3 - F_5 - F_8 + 3F_{11})$
$C_4 = 2\,(8F_1 - 4F_4 - F_6 + 4F_{10} + 3F_{12})$
$C_3 = 2\,(4F_2 + 4\,F_3 - F_5 + F_8 + 3F_{11})$
$C_2 = 2\,(2F_4 + 2F_7 + F_9 + 2F_{10} + 2F_{12})$
$C_1 = 2\,(F_5 + F_8 + F_{11})$
$C_0 = F_9 + F_6 + F_{12}.$ (32)

Thus an eight degree polynomial in the variable x_5, i.e. equation (31), can be obtained for each of the two sets of solutions for the sums θ_{1+2}, θ_{3+4}, and θ_{5+6}. Values of θ_5 are obtained from (31) for each of the eight solutions of the polynomial as

$$\theta_5 = 2\tan^{-1}(x_5). \tag{33}$$

Corresponding values of θ_6 are obtained from

$$\theta_6 = (\theta_5+\theta_6) - \theta_5. \tag{34}$$

3.5.3 Solution for θ_2, θ_1, and φ_1

Values for the angle θ_2 are now to be determined which correspond to each solution set of θ_5. The terms A_6, B_6, and D_6 are now defined in terms of known parameters as

$$A_6 = A_3c_5 + A_4s_5 + A_5 \tag{35}$$
$$B_6 = B_3c_5 + B_4s_5 + B_5 \tag{36}$$
$$D_6 = D_2s_5 + D_3. \tag{37}$$

Substituting these terms into (13), (14), and (15) gives

$$A_1c_2 + A_2c_3 + A_6 = 0 \tag{38}$$
$$B_1s_2 + B_2s_3 + B_6 = 0 \tag{39}$$
$$D_1s_2 + D_6 = 0. \tag{40}$$

The corresponding value for $\sin\theta_2$ can be obtained directly from (40) as

$$s_2 = \frac{-D_6}{D_1}. \tag{41}$$

The value for $\cos\theta_2$ will be obtained by writing (38) and (39) as

$$-c_3 = (A_1c_2 + A_6)/A_2, \tag{42}$$
$$-s_3 = (B_1s_2 + B_6)/B_2. \tag{43}$$

Squaring and adding these equations yields

$$\left(\frac{A_1c_2 + A_6}{A_2}\right)^2 + \left(\frac{B_1s_2 + B_6}{B_2}\right)^2 - 1 = 0. \tag{44}$$

Expanding this equation yields

$$\frac{A_1^2c_2^2 + 2A_1A_6c_2 + A_6^2}{A_2^2} + \frac{B_1^2s_2^2 + 2B_1B_6s_2 + B_6^2}{B_2^2} - 1 = 0. \tag{45}$$

Equation (41) may be used to directly substitute for s_2 in terms of known parameters. The term $\cos^2\theta_2$ may be replaced by squaring (41), substituting $c_2^2=1-s_2^2$, and solving for c_2^2 as

$$c_2^2 = 1 - \left(\frac{-D_6}{D_1}\right)^2. \tag{46}$$

Substituting (46) into (45) and solving for c_2 gives

$$c_2 = \frac{A_1^2A_{126} + A_2^2B_{126} - A_6^2B_2^2D_1^2}{2D_1^2B_2^2A_1A_6} \tag{47}$$

where:

$A_{126} = B_2^2D_6^2 - B_2^2D_1^2$

$B_{126} = D_1^2(B_2^2 - B_6^2) + 2B_1B_6D_1D_6 - B_1^2D_6^2.$

Knowledge of the sine and cosine of θ_2 from (41) and (47) gives a unique value for the angle θ_2. The corresponding value of the angle θ_1 is obtained from

$$\theta_1 = (\theta_1+\theta_2) - \theta_2. \tag{48}$$

Lastly, values for the first joint parameter, φ_1, are obtained from (6) as

$$\varphi_1 = \theta_1 - \gamma_1. \tag{49}$$

3.5.4 Solution for θ_3 and θ_4

The angles θ_3 and θ_4 are the last two remaining parameters to be obtained. The sine and cosine of θ_3 that correspond to each solution set of θ_1, θ_2, θ_5, and θ_6 can be obtained directly from (42) and (43) yielding a unique corresponding value for θ_3. The corresponding value for θ_4 is then obtained from

$$\theta_4 = (\theta_3 + \theta_4) - \theta_3. \tag{50}$$

At this point all the joint angle parameters have been obtained. Figure 6 illustrates the sixteen solutions.

4. NUMERICAL EXAMPLE

The constant mechanism parameters of an example case are presented in Table 1. The free choice values for the offset S_6, the hypothetical link length a_{67} and the hypothetical twist angle α_{67} are presented in Table 1. The position and orientation requirements are summarized in Table 2. The closed-the-loop parameters obtained for this case are summarized in Table 3.

The solution for the equivalent spherical quadrilateral for the sums $\theta_1+\theta_2$, $\theta_3+\theta_4$, and $\theta_5+\theta_6$ is presented in Table 4. Fourteen real solutions and two complex solutions were found for this numerical example and are summarized in Table 5.

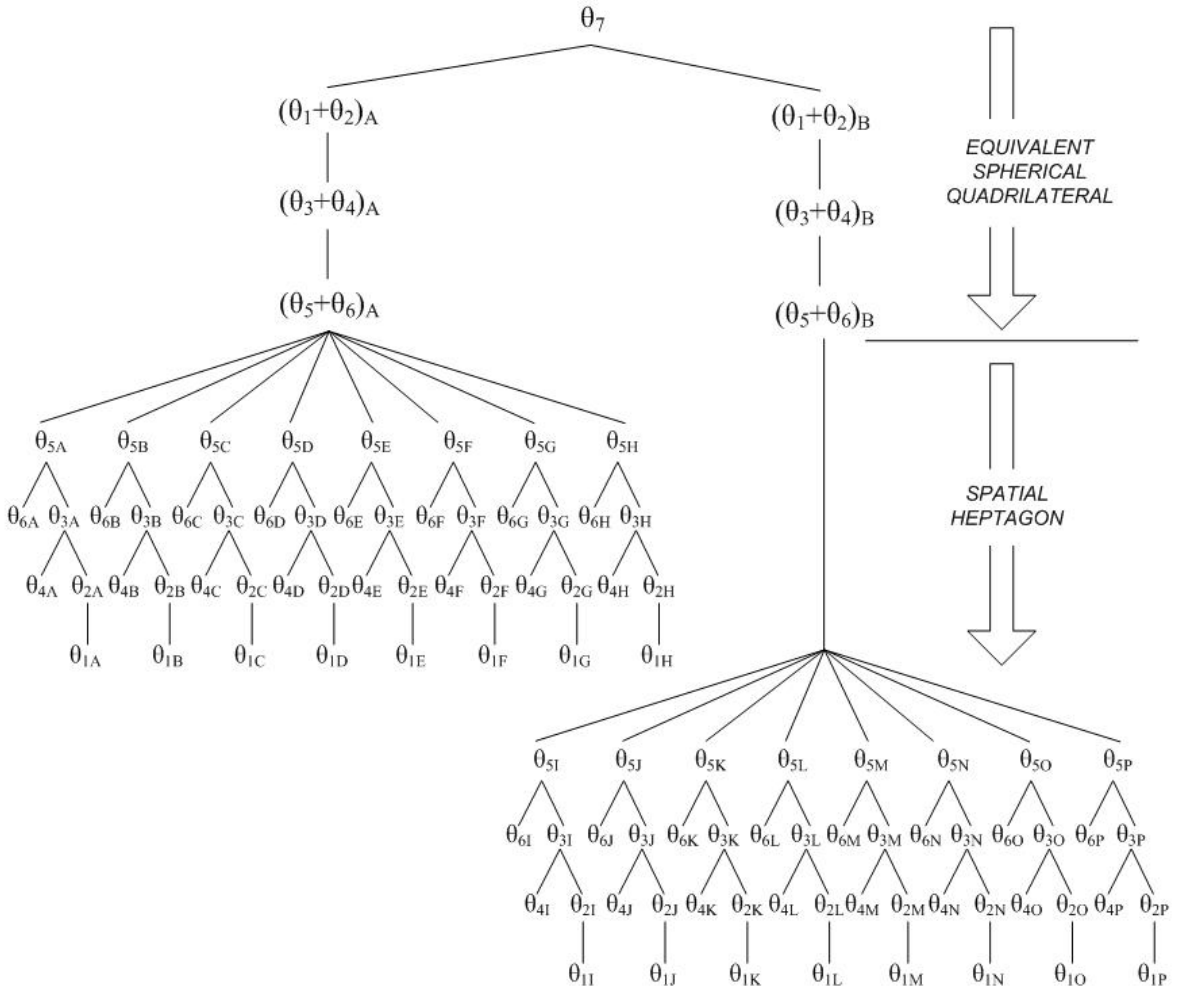

Figure 6: Solution tree for the spatial six axis manipulator with consecutive axes parallel.

Table 1: Constant mechanism parameters for numerical example

Offset Distance [in]	Link Lengths [in]	Twist Angles [deg]
$S_2 = 3.4947$	$a_{12} = 14.2368$	$\alpha_{12} = 0$
$S_3 = 0$	$a_{23} = 0.7411$	$\alpha_{23} = 59.2992$
$S_4 = 1.3465$	$a_{34} = 12.9009$	$\alpha_{34} = 0$
$S_5 = 0$	$a_{45} = 6.1349$	$\alpha_{45} = 76.8924$
$S_6^* = 6.0$	$a_{56} = 10.3782$	$\alpha_{56} = 0$
	$a_{67}^* = 0$	$\alpha_{67}^* = 90$

*: Free choice.

Table 2: Desired position and orientation

${}^F\mathbf{a}_{67}$	[-0.4771 -0.5994 -0.6428]
${}^F\mathbf{S}_6$	[0.7393 -0.6692 0.0752]
${}^F\mathbf{P}_{tool}$ [in]	[10.1041 -8.0151 0.5516]
${}^6\mathbf{P}_{tool}$ [in]	[5 7 8]

Table 3: Calculated close-the-loop parameters

Distance [in]	Angle [degrees]
$a_{71} = 4.2174$	$\alpha_{71} = 40.3277$
$S_7 = 0.8123$	$\theta_7 = -96.6756$
$S_1 = -9.119$	$\gamma_1 = -132.7510$

Table 4: Sums of consecutive joint angles obtained from the equivalent spherical quadrilateral solution

Sum of Angles	Solution A [degrees]	Solution B [degrees]
θ_{1+2}	-7.5924	-162.2098
θ_{3+4}	-87.2244	87.2244
θ_{5+6}	-80.4042	160.6752

Table 5: Joint angles corresponding to the sixteen solutions of the numerical example

Sol	φ_1[deg]	θ_2[deg]	θ_3[deg]	θ_4[deg]	θ_5[deg]	θ_6[deg]
A	119.6877	5.4709	177.7643	95.0113	-177.7795	97.3753
B	281.5373	-156.3786	-6.1702	-81.0542	145.8062	133.7896
C	155.4960	-30.3374	-175.0900	87.8656	136.4939	143.1019
D	-5.6494 +31.5413 i	130.8063 -31.5413 i	31.5585 +42.3301 i	-118.7799 -42.3301	-127.9873 +39.4481	47.5841 -39.4481
E	-5.6494 -31.5413 i	130.8063 +31.5413 i	31.5585 -42.3301 i	-118.7799 +42.3301	-127.9873 -39.4481	47.5841 +39.4481
F	174.3520	54.1905	114.2585	158.5171	-115.1178	34.7136
G	173.63906	-48.4804	149.8232	122.9524	79.5779	-159.9822
H	262.0020	-136.8434	47.4029	-134.6273	64.8370	-145.2412
I	129.0418	-158.5006	19.6492	67.5752	150.2720	10.4032
J	185.5112	145.0300	52.55648	34.6679	-140.0509	-59.2739
K	2.4264	-31.88519	172.7676	-85.5432	136.2312	24.4440
L	21.5798	-51.0386	-136.5833	-136.1922	83.5839	77.0913
M	100.3648	-129.8236	-47.9943	135.2187	79.1644	81.5108
N	270.2382	60.3030	159.7512	-72.5268	-89.8907	-109.4341
O	273.2697	57.2715	172.7296	-85.5052	-75.1938	-124.1310
P	171.1326	159.4086	-43.9788	131.2032	-21.9573	-177.3675

Figure 7 illustrates the fourteen real configurations for the open-loop manipulator in this numerical example. A forward analysis was performed as a check and all sixteen solutions, including the complex solutions, position and orient the end effector as desired.

`Efforts to identify a numerical example that would yield sixteen real solutions have not yet been successful. However, the fact that the two complex solutions in this example do satisfy the problem statement indicates that sixteen is the correct degree of the solution for this geometry.

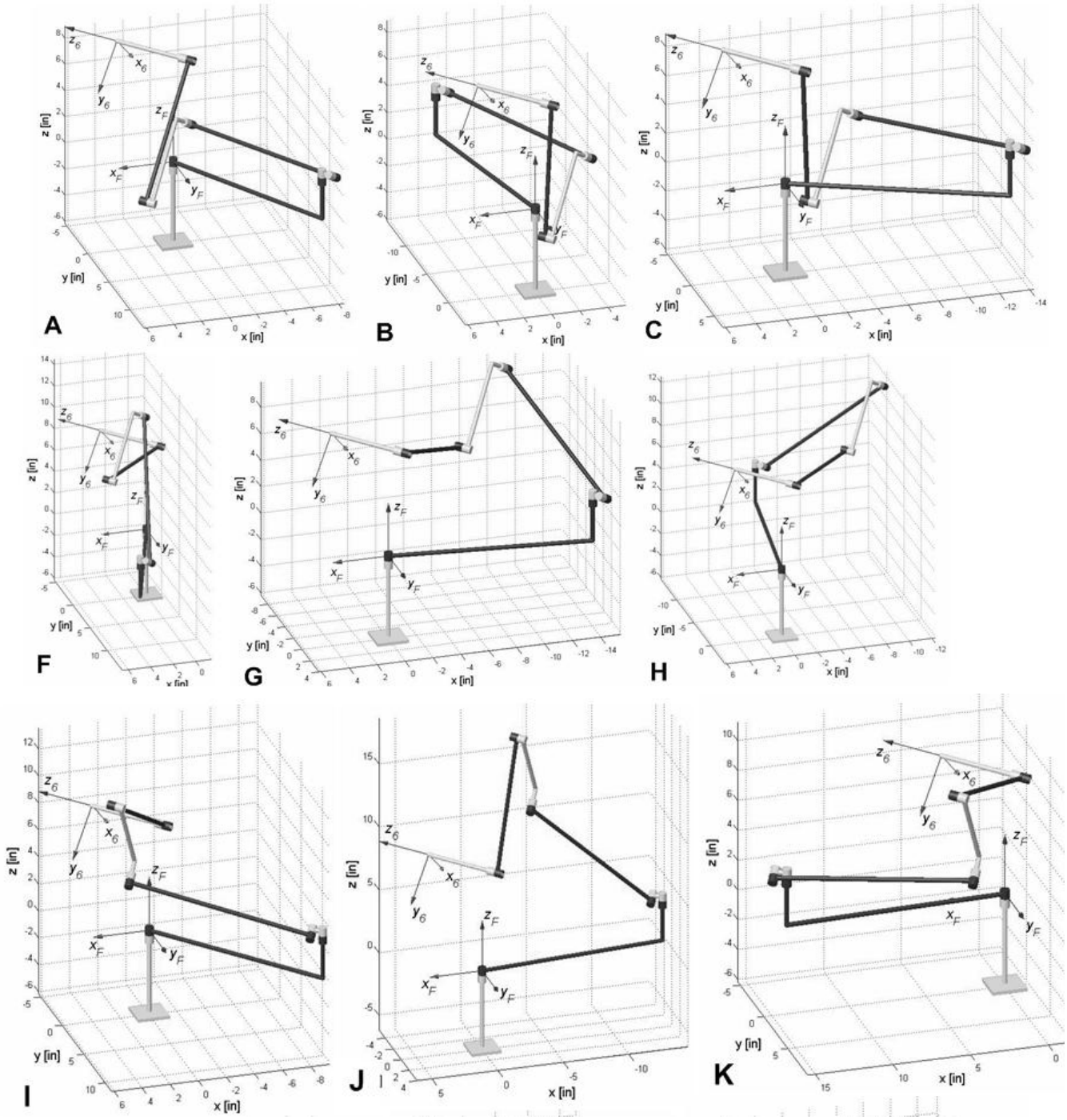

Figure 7: Fourteen real solutions in Table 5

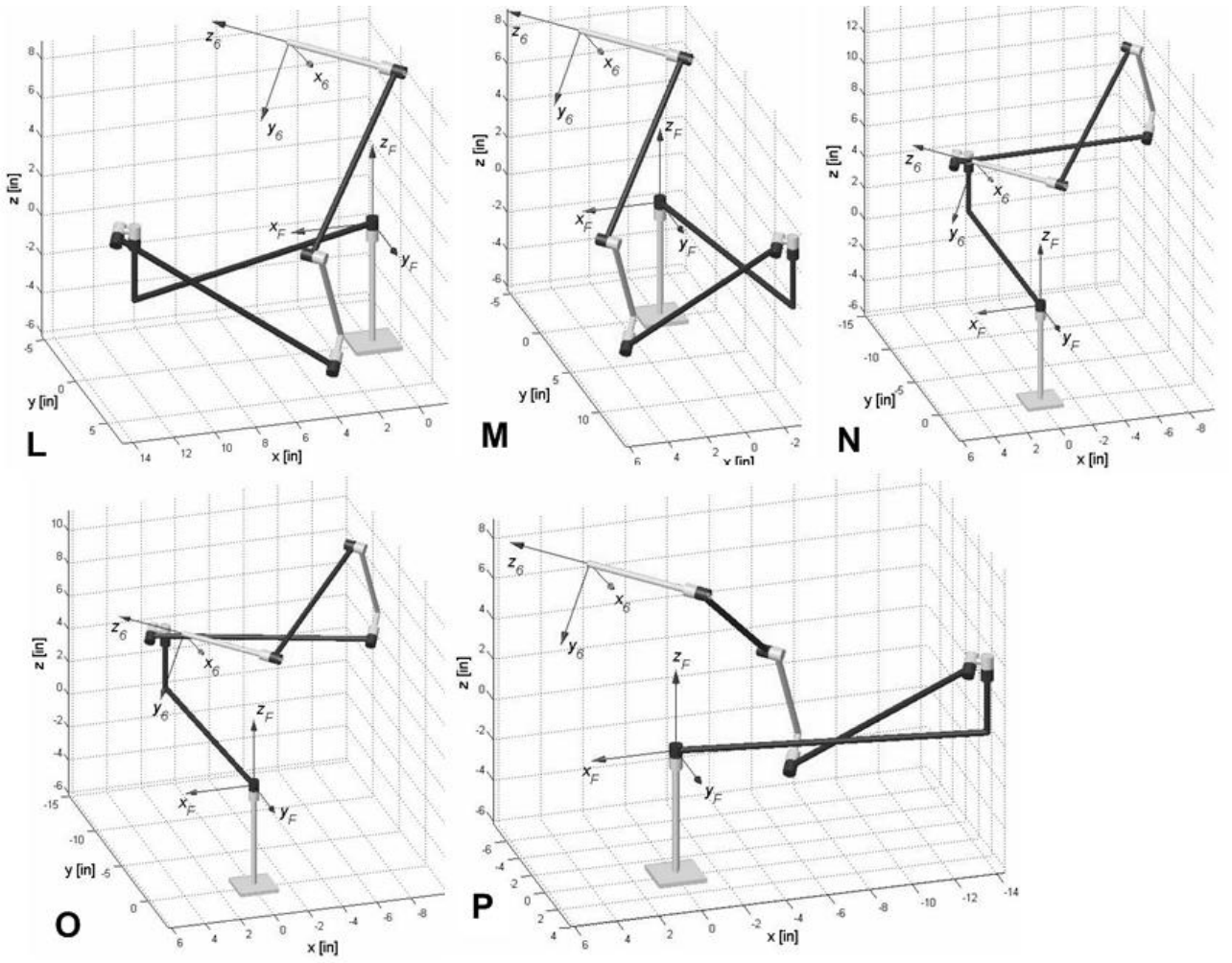

Figure 7: Fourteen real solutions in Table 5

5 CONCLUSION

The reverse kinematic solution of a spatial open-loop mechanism consisting of six revolute joints and six serial links, with consecutive pairs of joint axes parallel was presented in this paper. The solution technique incorporated a hypothetical closure-link to form a one degree-of-freedom closed-loop spatial mechanism where one of the joint angles, θ_7, is known. An analysis of the equivalent closed-loop spherical mechanism resulted in the solution of two sets of solutions for the joint angle sums $(\theta_1+\theta_2)$, $(\theta_3+\theta_4)$, and $(\theta_5+\theta_6)$. Projection of the vector loop equation of the spatial mechanisms on three independent directions then resulted in a set of equations from which a total of sixteen solution sets for the joint angles could be obtained. A numerical example was presented which verifies the degree of the solution.

The motivation of this work is related to future applications of spatial motion generation incorporating non-circular gears. Using the geometry discussed here, five pairs of planar non-circular gears can be incorporated into a spatial twelve axis closed-loop mechanism to result in a one degree-of-freedom device where the coupler link is positioned and oriented along a desired path. This problem is currently under investigation.

ACKNOWLEDGMENTS

The authors gratefully acknowledge the support provided by the Department of Energy via the University Research Program in Robotics (URPR), grant number DE-FG04-86NE37967.

REFERENCES

[1] Suh C. (1968), "Design of Space Mechanisms for Function Generation," Journal of Engineering for Industry, Trans. ASME, Vol. 90, Series B, No. 3, pp. 507-512.

[2] Suh C. (1968), "Design of Space Mechanisms for Rigid Body Guidance," Journal of Engineering for Industry, Trans. ASME, Vol. 90, Series B, No. 3, pp. 499-506.

[3] Rooney J., and Duffy J. (1972), "On the Closures of Spatial Mechanisms," Paper No. 72-Mech-77, Twelfth ASME Mechanisms Conference, Oct. 8.

[4] Duffy J., and Rooney J. (1974), "A Displacement Analysis of Spatial Six-Link 4R-P-C Mechanisms: Part 1: Analysis of RCRPRR Mechanism," Journal of Engineering for Industry, Trans, ASME, Vol. 96, Series B, No. 3, pp. 705-712.

[5] Duffy J., and Rooney J. (1974), "A Displacement Analysis of Spatial Six-Link 4R-P-C Mechanisms: Part 2: Derivation of the Input-Output Displacement Equation for RCRRPR Mechanism," Journal of Engineering for Industry, Trans, ASME, Series B, Vol. 96, No. 3, pp. 713-717.

[6] Duffy J., and Rooney J. (1974), "A Displacement Analysis of Spatial Six-Link 4R-P-C Mechanisms: Part 3: Derivation of Input-Output Displacement Equation for RRRPCR Mechanism," Journal of Engineering for Industry, Trans, ASME, Series B, Vol. 96, No. 3, pp. 718-721.

[7] Duffy J., and Rooney J. (1974), "Displacement Analysis of Spatial Six-Link 5R-C Mechanisms," Journal of Applied Mechanics, Trans. ASME, Vol. 41, Series E, No. 3, pp. 759-766.

[8] Duffy J. (1977), "Displacement Analysis of Spatial Seven-Link 5R-2P Mechanisms," Journal of Engineering for Industry, Trans, ASME, Vol. 99, Series B, No. 3, pp. 692-701.

[9] Sandor G., Kohli D., and Zhuang X. (1985), "Synthesis of RSSR-SRR Spatial Motion Generator Mechanism with Prescribed Crank Rotations for Three and Four Finite Positions," Mechanism and Machine Theory, Vol. 20, No. 6, pp. 503-519.

[10] Sandor G., Yang S., Xu L., and De, P. (1986), "Spatial Kinematic Synthesis of Adaptive Hard-Automation Modules: An RS-SRR-SS Adjustable Spatial Motion Generation," Journal of Mechanisms, Transmissions, and Automation Design, Trans. ASME, Vol. 108, pp. 292-299.

[11] Lee H., and Liang C. (1987), "Displacement Analysis of the Spatial 7-Link 6R-P linkages," Mechanism and Machine Theory, Vol. 22, No. 1, pp. 1-11.

[12] Dhall S., and Kramer S. (1988), "Computer-Aided Design of the RSSR Function Generating Spatial Mechanism Using the Selective Precision Synthesis Method," Journal of Mechanisms, Transmissions, and Automation Design, Trans. ASME, Vol. 110, pp. 378-382.

[13] Premkumar P., and Kramer S. (1989), "Position, Velocity, and Acceleration Synthesis of the RRSS Spatial Path-Generating Mechanism Using the Selective Precision Synthesis Method," Journal of Mechanisms, Transmissions, and Automation Design, Trans. ASME, Vol. 111, pp. 54-58.

[14] Dhall S., and Kramer S. (1990), "Design and Analysis of the HCCC, RCCC, and PCCC Spatial Mechanism for Function Generation," Journal of Mechanical Design, Trans. ASME, Vol. 112, pp. 74-78.

[15] Duffy J., and Rooney J. (1975), "A Foundation for a Unified Theory of Analysis of Spatial Mechanisms", Journal of Engineering for Industry, Trans. ASME, Vol. 97, Series B, No. 4, pp. 1159-1164.

[16] Crane III C., and Duffy J. (1998), *Kinematic Analysis of Robot Manipulators*, Cambridge University Press, USA.

[17] Ritcher S. L., and DeCarlo R. A. (1983), "Continuation Methods: Theory and Applications," IEEE Transactions on Circuits and Systems, Vol. CAS-30, No. 6, pp. 347-352.

[18] Sommese A. J., Verschelde J., and Wampler C. W. (2004), "Advances in Polynomial Continuation for Solving Problems in Kinematics," Journal of Mechanical Design, Trans. ASME, Vol. 126, pp. 262-268.

[19] Mu Z., and Kazerounian K. (2002), "A Real Parameter Continuation Method for Complete Solution of Forward Position Analysis of the General Stewart," Journal of Mechanical Design, Trans. ASME, Vol. 124, pp. 236-244.

[20] Nielsen J., and Roth B. (1999), "On the Kinematic Analysis of Robotic Mechanisms," The International Journal of Robotics Research, Vol. 18, No. 12, pp. 1147-1160.

[21] Angeles J. (1997), *Fundamentals of Robotic Mechanical Systems. Theory, Methods and Algorithms*, Springer, NY.

[22] Duffy J., and Crane C. (1980), "A Displacement Analysis of the General Spatial 7-Link, 7-R Mechanism," Mechanism and Machine Theory, Vol. 15, No. 15, pp. 153-169.

[23] Lee H., and Liang C. (1988), "Displacement Analysis of the General Spatial 7-Link 7-R Mechanism," Mechanism and Machine Theory, Vol. 23, No. 3, pp. 219-226.

[24] Husty M., Pfurner M., and Schröcker H-P. (2006), "A New and Efficient Algorithm for the Inverse Kinematics of a General Serial 6R Manipulator," Mechanism and Machine Theory, Vol. 42, No. 1, pp. 66-81.

[25] Roldán McKinley J., Dooner D., Crane III C., and Kamath J. (2005), "Planar Motion Generation Incorporating a 6-Link Mechanism and Non-Circular Elements," Paper DETC2005-85315, ASME 29th Mechanism and Robotics Conference, Sept. 24-28, 2005 Long Beach, CA.

[26] Real Diez-Martinez C., Rico J., Cervantes-Sánchez J., and Gallardo J. (2006), "Mobility and Connectivity in Multiloop Linkages," pp. 455-464, in *Advances in Robot Kinematics*, Springer, Netherlands.